Temperature Coefficient of Resistance of Transferred Laser-Induced Graphene

Yanpeng Li[1†], Haruki Nakamura[1†], Do Hoon Lee[1], Yue Qin[1], Yan Xuan[1], Kuniharu Takei[1]*

[1]Graduate School of Information Science and Technology, Hokkaido University, Sapporo, Hokkaido 060-0814, Japan

*Corresponding author: takei@ist.hokudai.ac.jp

[†]These authors equally contributed.

Keywords: Laser-induced graphene, TCR, temperature sensor, elastomer, strain sensor

Abstract: Laser-induced graphene (LIG) has attracted considerable attention as an electrode and sensor in flexible and stretchable devices. For instance, resistive temperature sensors have been developed using a LIG conductor as an active component. However, despite the evidence that LIG can be used as a temperature sensor, fundamental analyses confirming LIG as a temperature sensor material are still required. Therefore, this study investigates the temperature coefficient of resistance (TCR) of a transferred LIG in stretchable elastomers. To remove the effect of thermal expansion of elastomers, elastomers with different coefficient of thermal expansion (CTE) values are used, and the temperature responses of LIG in these elastomers are measured. Furthermore, to calibrate the resistance change caused by thermal expansion-induced strain, strain effects are characterized by stretching the films. Combining the results reveal that the TCR of the transferred

LIG was ca. −0.44%/°C and the sensitivity depended on LIG depth location.

INTRODUCTION

Laser-induced graphene (LIG) can be used as an electrode and sensor in flexible and stretchable electronics owing to its simple fabrication process; it is highly scalable for macroscale electronics. LIG is formed via laser scanning on a polyimide (PI) film[1], which is converted into a randomly formed graphene layer with a porous structure under the action of heat induced by the laser exposure[2]. This unique and highly conductive structure of graphene allows its application to functional materials such as those used in sensors[3-11]. Another advantage of LIG is that it can be easily transferred onto solution-based elastomers by coating a precursor of the elastomer on a LIG/PI film, followed by curing and delaminating it from the PI film. Because the solution-based elastomer can penetrate into the porous LIG structure, LIG is embedded and readily transferred in the elastomer after curing. Using these LIG-embedded films, a strain sensor was developed, which operates on the basis of changes in the density of LIG under strain, resulting in a change in the LIG resistance as a function of strain[12-15]. The application of LIG as a temperature sensor has also been demonstrated[5, 8, 16]. Owing to the temperature coefficient of resistance (TCR) of LIG and the thermal expansion of film substrates, changes in temperature cause a resistance change. However, the origin of the TCR of LIG remains unveiled because flexible films often have a large

coefficient of thermal expansion (CTE), and a systematic study on the fundamental temperature property of LIG is required. To this aim, this study investigates the TCR of transferred LIG (TCR_{LIG}) by measuring the temperature characteristics and strain dependence while removing the CTE effect of the film using different stretchable films. The results on TCR confirmed that the resistance change depends on the location of LIG on the PI film because the density of LIG changes upon laser exposure. By assuming that TCR_{LIG} is constant and only CTE changes depending on the elastomer, the thermal expansion effect can be removed to systematically study TCR_{LIG} (Figure 1a).

RESULTS AND DISCUSSION

The fabrication process is briefly explained in Figure 1b. First, a PI film was prepared (Figure 1b(1)) and subjected to laser scanning to form LIG (Figure 1b(2)) [14, 17]. Then, elastomer precursors were poured over the LIG/PI film and cured to form the elastomers (Figure 1b(3)). Details of the elastomers and process conditions are given in the Methods section. Next, the elastomer film with LIG was delaminated from the PI film. After the transferring process, almost all LIG was transferred into the elastomers. In order to use the same quality of LIG for the characterizations, it was confirmed that all LIGs on the PI films formed by the same laser condition were fully transferred in the elastomer films, and there is virtually no residue left on the PI film. To ensure the stability of the electrical measurements to determine the temperature and strain effects on the

LIG film, GaInSn liquid metal was printed over silver (Ag) to prepare interconnected electrodes. Owing to its low resistance (~1.5 Ω) compared to LIG (~70 Ω to 1.1 kΩ depending on the substrate) and liquid state, GaInSn can be used as the electrode without affecting the output resistance change even under stretching. As stretchable elastomer films, we selected a thermoplastic polyurethane (TPU) 90A, Ecoflex, and a polydimethylsiloxane (PDMS) with CTE values of 190, 284.2, and 300 ppm/°C, respectively (Figure 1c). The cross-sectional scanning electron microscopy (SEM) shown in Figure 1d reveals that ~200-μm-thick LIG is embedded in each stretchable elastomer. To confirm the quality of LIG before and after the transfer into the elastomer, Raman spectroscopy was conducted. All transferred LIGs in the stretchable elastomers exhibit amorphous-like nanocarbon structures having broad D and G peaks and no 2D peak, whereas the Raman spectrum of LIG before transfer shows clear 2D, G, and D peaks (Figure 1e). These results are in accord with previous reports[14, 17]. The reason for these changes in the Raman spectra after the transfer process remains unknown and should be the subject of future studies; however, it is beyond the scope of this study, which aims to determine the TCR of LIG. Although the mechanism of this crystallinity change is still unknown, it reveals that all transferred LIGs are similar crystal quality to discuss TCR.

Temperature dependence studies were performed by measuring the resistance at different temperatures ranging from 30°C to 90°C. The resistance change ratio ($\Delta R/R_0$) was calculated

from the resistance difference (ΔR) at the measured temperature and the initial resistance (R_0) at 30°C. The measurements were conducted in an environmental control oven at a constant relative humidity of 40% (Figure 2a–d). As a reference, LIG on the PI sample was also subjected to these measurements (Figure 2a). Interestingly, using low-CTE films including the PI film, the resistance decreased with increasing temperature, whereas the resistance increased with temperature, when high-CTE films PDMS and Ecoflex were used. These different trends suggest that thermal expansion cannot be ignored to determine the TCR of LIG or to design a flexible temperature sensor. Figure 2e displays the resistance change ratio as a function of temperature, revealing clearly different trends, i.e., negative and positive resistance changes, with increasing temperature depending on the elastomer. Importantly, all resistance change ratio–temperature plots could be linearly fitted, which allowed calculating the sensitivity corresponding to TCR using the linear fitting. More than 10 samples were measured for each material (see Figure 1c for the specific sample numbers). The results depicted in Figure 2f show no trend between TCR and CTE. To ensure a consistent device structure and material quality (i.e. amorphous) for an accurate comparison, the LIG/PI sample was excluded for subsequent analysis.

The temperature dependence results clearly reveal that TCR of LIG and thermal expansion of the film affect the resistance change of LIG in elastomer films. To compensate the thermal expansion of the film, which is related to strain, strain dependences were characterized by

stretching the film up to 20% tensile strain (Figure 3a–c). After measuring the resistance change ratio as a function of strain for each elastomer film, the strain sensitivities were calculated from the linear fitting of the resistance change ratio ($\Delta R/R_0$), where R_0 is the resistance before applying strain and ΔR is the resistance change from R_0. (Figure 3d). LIG/PDMS and LIG/TPU 90A show similar sensitivities, i.e., $S_{LIG/PDMS}$ = 0.934 %/% and $S_{LIG/TPU}$ = 1.128 %/%. In contrast, the sensitivity of LIG/Ecoflex ($S_{LIG/Ecoflex}$ ~ 2.015 %/%) is almost double than those of LIG/PDMS and LIG/TPU 90A. Similar sensitivity from more than two samples for each material was confirmed. Therefore, the strain sensitivity must be considered to determine the TCR of transferred LIG. In this study, strain caused by thermal expansion could not be directly observed due to small strain change under temperature change used. To understand the strain effect of LIG in elastomer films caused by temperature change, a scanning electron microscopy or a transmission electron microscopy with a heating function is required to observe the strain in LIG caused by heating. This detail study should be conducted in the future to understand LIG, which is beyond our scope of this study.

The TCR of transferred LIG without any thermal expansion effect was examined according to the results of the temperature and strain dependences. Due to TCR of LIG and thermal expansion of the elastomer film, temperature sensitivity S_1 is expressed as:

$$S_1 = \alpha\,\mathrm{CTE} + TCR_{LIG} \quad (1)$$

where α is proportional coefficient that depends on elastomer, CTE is CTE value of elastomer, and TCR_{LIG} is TCR value of LIG. Since α is the coefficient of strain caused by thermal expansion, α_{PDMS}, α_{TPU}, and $\alpha_{Ecoflex}$ are related to the strain sensitivity extracted in Figure 3d, and the following relation can be expected.

$$\alpha_{PDMS}: \alpha_{TPU}: \alpha_{Ecoflex} = S_{LIG/PDMS}: S_{\mathrm{LIG/TPU}}: S_{\mathrm{LIG/Ecoflex}} = 0.934: 1.128: 2.015 \quad (2)$$

From equations (1) and (2), following equations were derived.

$$S_{1_{PDMS}} = \alpha_{PDMS}\, CTE_{PDMS} + TCR_{LIG} \quad (3)$$

$$S_{1_{TPU}} = \frac{1.128}{0.934}\alpha_{PDMS} CTE_{TPU} + TCR_{LIG} \quad (4)$$

$$S_{1_{Ecoflex}} = \frac{2.015}{0.934}\alpha_{PDMS}\, CTE_{Ecoflex} + TCR_{LIG} \quad (5)$$

CTE_{PDMS}, CTE_{TPU}, and $CTE_{Ecoflex}$ are CTE values of each elastomer film. To calculate TCR_{LIG} from these equations, combinatorial optimization to α_{PDMS} and TCR_{LIG} was applied. Optimization was performed by calculating S_1 values of each elastomer film using CTE values and arbitrary α_{PDMS} and TCR_{LIG}. For evaluation, Normalized Mean Squared Error (NMSE) was used according to the following formula.

$$NMSE = \frac{1}{N \times \sigma}\sum (S_1 - y)^2 \quad (6)$$

N is the number of data, σ is the variance of S_1, and y is temperature sensitivity calculated by equation (3)-(5). The average of NMSE ($NMSE_{average}$) was calculated using the following formula (7), and the combination with the smallest $NMSE_{average}$ value was selected as the optimal

combination.

$$NMSE_{average} = \frac{1}{3}\left(NMSE_{PDMS} + NMSE_{TPU} + NMSE_{Ecoflex}\right) \quad (7)$$

As a result of computational calculation, the optimal combination was found to be α_{PDMS}= 0.0017 and $TCR_{LIG} = -0.44$. Despite the large deviation due to the variation of the results of PDMS and Ecoflex, the TCR of the transferred LIG was determined to be ca. −0.44 %/°C. The fact that it is a negative temperature coefficient (NTC) suggests that LIG exhibits semiconductor-like characteristics in terms of the temperature response. The negative TCR value explains the trend difference of resistance change, which resistance of LIG in a small CTE material such as TPU 90A decreases while those of LIG in PDMS and Ecoflex with relatively large CTEs increases by increasing temperature as shown in Figure 2e.

To gain a deeper understanding of the temperature effect on LIG, LIG was sandwiched between PI and PDMS without transfer, as described in Figure 4a. The cross-sectional SEM image shown in Figure 4b reveals that LIG on PI has nonporous and porous regions. Furthermore, the porous structure of LIG can be clearly observed in the top view of the SEM image (Figure 4c). After producing LIG on the PI film, PDMS was formed over the resulting LIG/PI. Owing to the presence of two layers of LIGs with different densities (porous and nonporous), the effect of strain caused by thermal expansion on each layer was analyzed although the density difference cannot be quantitatively determined. To this aim, the electrical resistance without delamination of the

PDMS layer from the PI film was measured. LIG/PI has a negative resistance change mainly caused by TCR, whereas LIG/PDMS has a positive resistance change induced by thermal expansion with increasing temperature (Figure 2a and d). Accordingly, measuring the resistance change caused by thermal expansion of PI (ΔR_{PI_CTE}) and PDMS (ΔR_{PDMS_CTE}) and the TCR of LIG (ΔR_{LIG_TCR}) should reveal the main region undergoing the resistance change against strain caused by the temperature change. As a result, the resistance change ratio decreases when the temperature increases (Figure 4d and e). From the linear fitting of the resistance change ratio, sensitivity was determined to be ca. −0.025%/°C. In accordance with the NTC characteristics, this sensitivity is lower than that of PI/LIG without PDMS (ca. −0.046%/°C, Figure 2e). Notably, the TCR of LIG extracted from the calculation cannot be used for this comparison because PI/LIG was excluded from TCR estimation owing to process and material differences. However, it can be concluded that nonporous LIG exhibits a stronger strain response than porous LIG, although there is a small influence of resistance change in the porous region.

CONCLUSIONS

In this study, the TCR of transferred LIG was investigated in the context of the design of a temperature sensor. By characterizing the temperature and strain effects on LIG embedded in different elastomer films, TCR was estimated to be ca. −0.44 %/°C without thermal expansion. It

is also revealed that selecting the elastomer material as a substrate is important to obtain negative and positive temperature coefficients. Furthermore, the sensitivity was found to depend on the depth location, which in turn is related to the LIG density. These fundamental studies on the LIG characteristics will contribute to the design of temperature sensors in the near future.

MATERIALS AND METHODS

Material preparation: The elastomer films were prepared as follows. SILPOT 184 was used as the PDMS precursors. PDMS base solution and a curing agent were mixed with a 10:1 wt.% ratio, and the PDMS films were obtained after curing at 90°C for more than 2 h. For the Ecoflex film, Ecoflex 00-30A with a 1:1 wt.% ratio (base and curing agent solutions) was used. The curing process was performed at 90°C for more than 20 min. For TPU 90A, TPU 90A pallets were first dissolved in dimethylformamide at a concentration of 200 mg/mL, and the film was prepared by curing at room temperature in air for more than 10 h.

Device fabrication: A CO_2 laser (VLS2.30, UNIVERSAL Laser System) with a power of 10 W (laser power:40%, laser speed:30% and the image density is 5) was used to form LIG on 125 μm-thick PI film. Next, the LIG/PI film was fixed in a mold with a depth of 2 mm using a double-side tape, and the elastic precursors were poured into the mold and cured to form elastomer films. The thicknesses of cured PDMS and Ecoflex films were ~2 mm while that of TPU 90A was ~1.5

mm. After transferring LIG to the elastomer films, Ag electrodes (~1 Ω) were printed on the contact region of LIG to make a stable electrical connection between the stretchable GaInSn liquid metal and LIG. Subsequently, GaInSn electrodes as flexible and stretchable electrodes were manually patterned using a syringe over the Ag electrodes. To monitor the resistance change using a datalogger, electrical wires were attached to the GaInSn electrodes and connected to the datalogger.

ASSCIATED CONTENT

Author Information

Corresponding Authors

Kuniharu Takei – Graduate School of Information Science and Technology, Hokkaido University, Sapporo 060-0814, Japan; Email: takei@ist.hokudai.ac.jp

Authors

Yanpeng Li – Graduate School of Information Science and Technology, Hokkaido University, Sapporo 060-0814, Japan,

Haruki Nakamura – Graduate School of Information Science and Technology, Hokkaido University, Sapporo 060-0814, Japan,

Do Hoon Lee – Graduate School of Information Science and Technology, Hokkaido University, Sapporo 060-0814, Japan,

Yue Qin – Graduate School of Information Science and Technology, Hokkaido University, Sapporo 060-0814, Japan,

Yan Xuan – Graduate School of Information Science and Technology, Hokkaido University, Sapporo 060-0814, Japan,

Author Contributions

†Y. L. and H. N. authors contributed equally to this work

Notes

The authors declare no competing financial interest.

ACKNOWLEDGEMENTS

This work was partially supported by JST AIP Accelerated Program (No. JPMJCR21U1), JSPS KAKENHI (Grant No. JP22H00594 and JP23KJ1841), the Murata Science Foundation, the Hitachi Global Foundation, and the Takeda Science Foundation.Y. Q. was supported by the China Scholarship Council, and Y. X. was supported by the JSPS Research Fellowships for Young Scientists (DC2).

REFERENCES

(1) Lin, J.; Peng, Z.; Liu, Y.; Ruiz-Zepeda, F.; Ye, R.; Samuel, E. L.; Yacaman, M. J.; Yakobson, B. I.; Tour, J. M. Laser-Induced Porous Graphene Films from Commercial Polymers. *Nat. Commun.* 2014, *5*, 5714.

(2) Ye, R.; James, D. K.; Tour, J. M. Laser-Induced Graphene. *Acc. Chem. Res.* **2018**, *51*, 1609-1620.

(3) Carvalho, A. F.; Fernandes, A. J. S.; Leitão, C.; Deuermeier, J.; Marques, A. C.; Martins, R.; Fortunato, E.; Costa, F. M. Laser-Induced Graphene Strain Sensors Produced by Ultraviolet Irradiation of Polyimide. *Adv. Funct. Mater.* **2018**, *28*, 1805271.

(4) Babatain, W.; Buttner, U.; El-Atab, N.; Hussain, M. M. Graphene and Liquid Metal Integrated Multifunctional Wearable Platform for Monitoring Motion and Human-Machine Interfacing. *ACS Nano* **2022**, *16*, 20305-20317.

(5) Yang, Y.; Song, Y.; Bo, X.; Min, J.; Pak, O. S.; Zhu, L.; Wang, M.; Tu, J.; Kogan, A.; Zhang, H.; Hsiai, T. K.; Li, Z.; Gao, W. A Laser-Engraved Wearable Sensor for Sensitive Detection of Uric Acid and Tyrosine in Sweat. *Nat. Biotech.* **2019**, *38*, 217-224.

(6) Lu, Y.; Kong, D.; Yang, G.; Wang, R.; Pang, G.; Luo, H.; Yang, H.; Xu, K. Machine Learning-Enabled Tactile Sensor Design for Dynamic Touch Decoding. *Adv. Sci.* **2023**, *10*, e2303949.

(7) Sharma, S.; Pradhan, G. B.; Jeong, S.; Zhang, S.; Song, H.; Park, J. Y. Stretchable and All-Directional Strain-Insensitive Electronic Glove for Robotic Skins and Human-Machine Interfacing. *ACS Nano* **2023**, *17*, 8355-8366.
(8) Lu, Y.; Yang, G.; Wang, S.; Zhang, Y.; Jian, Y.; He, L.; Yu, T.; Luo, H.; Kong, D.; Xianyu, Y.; Liang, B.; Liu, T.; Ouyang, X,; Yu, J.; Hu, X.; Yang, H.; Gu, Z.; Huang, W.; Xu, K. Stretchable Graphene–Hydrogel Interfaces for Wearable and Implantable Bioelectronics. *Nat. Electron.* **2023**, *7*, 51-65.
(9) Luo, H.; Lu, Y.; Xu, Y.; Yang, G.; Cui, S.; Han, D.; Zhou, Q.; Ouyang, X.; Yang, H.; Cheng, T.; Xu, K. A Fully Soft, Self-Powered Vibration Sensor by Laser Direct Writing. *Nano Energy* **2022**, *103*.
(10) Xiang, Z.; Wang, H.; Zhao, P.; Fa, X.; Wan, J.; Wang, Y.; Xu, C.; Yao, S.; Zhao, W.; Zhang, H.; Han, M. Hard Magnetic Graphene Nanocomposite for Multimodal, Reconfigurable Soft Electronics. *Adv. Mater.* **2024**, *36*, e2308575.
(11) Xu, K.; Li, Q.; Lu, Y.; Luo, H.; Jian, Y.; Li, D.; Kong, D.; Wang, R.; Tan, J.; Cai, Z.; Yang, G.; Zhu, B.; Ye, Q.; Yang, H.; Li, T. Laser Direct Writing of Flexible Thermal Flow Sensors. *Nano Lett.* **2023**, *23*, 10317-10325.
(12) Luong, D. X.; Subramanian, A. K.; Silva, G. A. L.; Yoon, J.; Cofer, S.; Yang, K.; Owuor, P. S.; Wang, T.; Wang, Z.; Lou, J.; Ajayan, P. M.; Tour, J. M. Laminated Object Manufacturing of 3D-Printed Laser-Induced Graphene Foams. *Adv. Mmater.* **2018**, *30*, e1707416.
(13) Sun, B.; McCay, R. N.; Goswami, S.; Xu, Y.; Zhang, C.; Ling, Y.; Lin, J.; Yan, Z. Gas-Permeable, Multifunctional On-Skin Electronics Based on Laser-Induced Porous Graphene and Sugar-Templated Elastomer Sponges. *Adv. Mater.* **2018**, *30*, 1804327.
(14) Xu, K.; Fujita, Y.; Lu, Y.; Honda, S.; Shiomi, M.; Arie, T.; Akita, S.; Takei, K. A Wearable Body Condition Sensor System with Wireless Feedback Alarm Functions. *Adv. Mater.* **2021**, *33*, e2008701.
(15) Li, Y.; Matsumura, G.; Xuan, Y.; Honda, S.; Takei, K. Stretchable Electronic Skin Using Laser-Induced Graphene and Liquid Metal With an Action Recognition System Powered by Machine Learning. *Adv. Funct. Mater.* **2024**, 2313824. DOI: 10.1002/adfm.202313824.
(16) Xu, C.; Song, Y.; Sempionatto, J. R.; Solomon, S. A.; Yu, Y.; Nyein, H. Y. Y.; Tay, R. Y.; Li, J.; Heng, W.; Min, J.; Lao, A.; Hsiai, T. K.; Sumner, J. A.; Gao, W. A Physicochemical-Sensing Electronic Skin for Stress Response Monitoring. *Nat. Electron.* **2024**, *7*, 168-179.
(17) Wakabayashi, S.; Arie, T.; Akita, S.; Nakajima, K.; Takei, K. A Multitasking Flexible Sensor via Reservoir Computing. *Adv. Mater.* **2022**, *34*, 2201663.

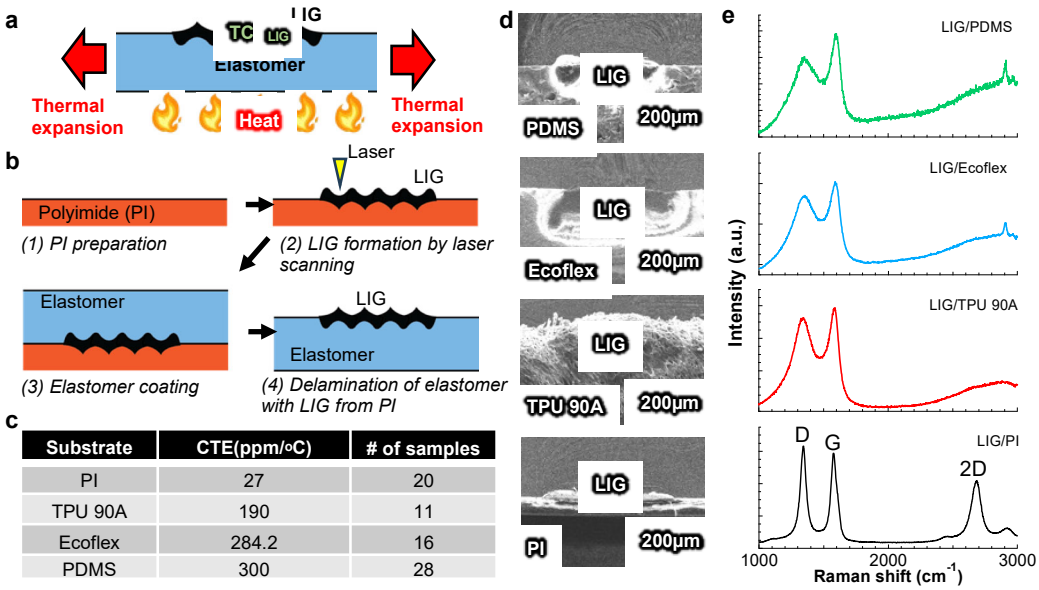

Substrate	CTE(ppm/°C)	# of samples
PI	27	20
TPU 90A	190	11
Ecoflex	284.2	16
PDMS	300	28

Figure 1. (a) Schematic of the concept to determine the temperature coefficient of resistance (TCR) of transferred laser-induced graphene (LIG) and thermal expansion of the films. (b) Schematic of the fabrication of the LIG/elastomer structure. (c) Coefficient of thermal expansion (CTE) and number of samples measured in this study for each elastomer film. (d) Cross-section SEM images and (e) Raman spectroscopy of LIG in PDMS, Ecoflex, TPU 90A, and polyimide (PI) films.

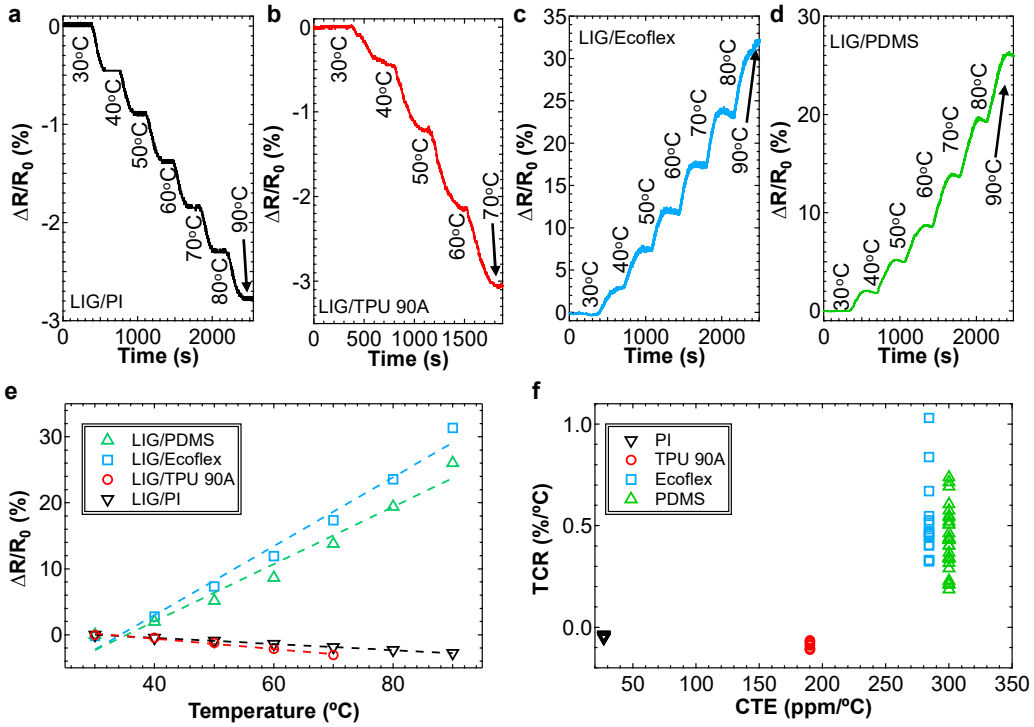

Figure 2. Resistance change ratio at different temperatures of (a) LIG/PI, (b) LIG/TPU 90A, (c) LIG/Ecoflex, and (d) LIG/PDMS. (e) Resistance change ratio as a function of temperature plotted from the results in (a–d). Dashed lines are extracted by line fitting. (f) Sensitivity at different CTE values. The sensitivity is calculated from the slopes of the line fitting results shown in (e).

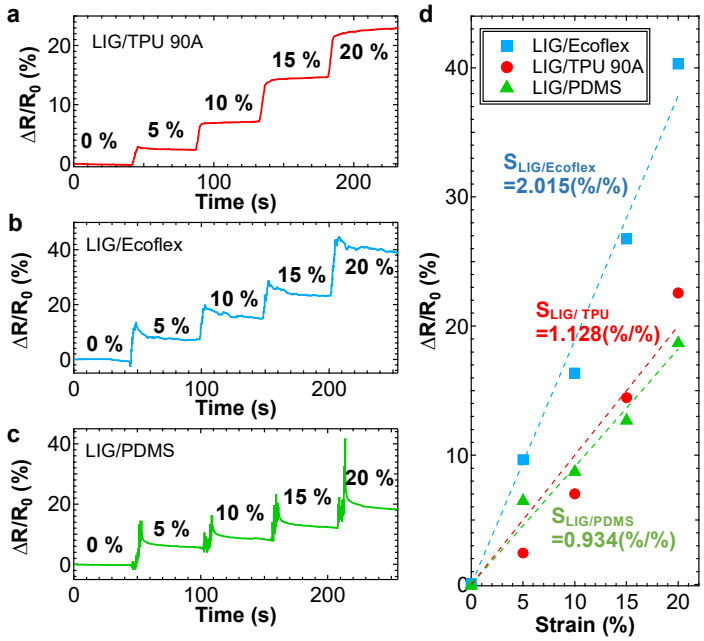

Figure 3. Stretching strain dependences of transferred LIG in (a) TPU 90A, (b) Ecoflex, and (c) PDMS. (d) Resistance change ratio of different elastomers as a function of strain with linear fitting results to determine the strain sensitivity.

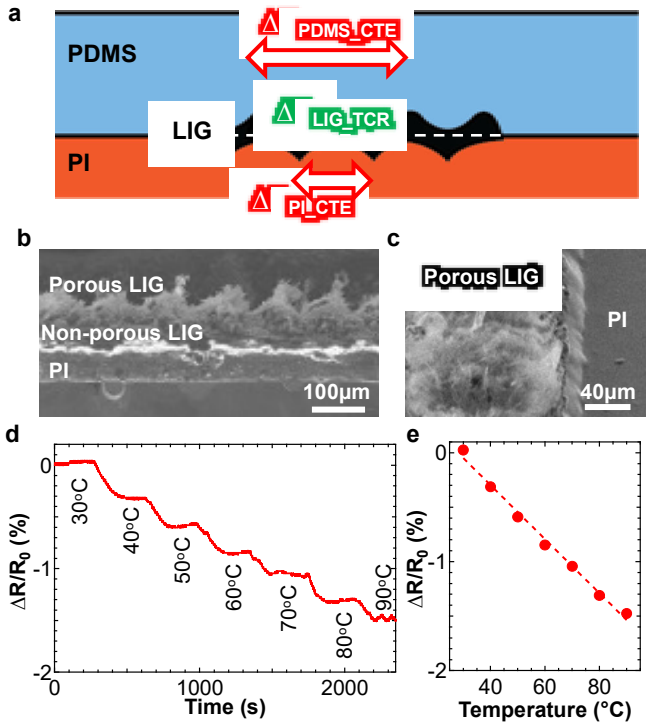

Figure 4. (a) Schematic image of LIG sandwiched between PDMS and PI. (b) Cross-sectional SEM image of LIG on PI. (c) Top view of SEM image of porous LIG on PI. (d) Resistance change ratio at different temperatures from the structure described in (a). (e) Resistance change ratio as a function of temperature extracted from (d).

For Table of Contents Use Only.